

Thermal and Combustion Properties of Energetic Thin Films with Carbon Nanotubes

Dylan K. Smith,* Jesus Cano,† and Michelle L. Pantoya‡

Texas Tech University, Lubbock, Texas 79409

and

Keerti Kappagantula§

Ohio University, Athens, Ohio 45701

DOI: 10.2514/1.T5009

The effect of varying carbon nanotube concentration on ignition delay, flame speed, and electrical and thermal conductivity of three-dimensional printable energetic thin films made of magnesium and manganese oxide was investigated. Polyvinylidene fluoride was used as the binder for depositing the stoichiometric Mg/MnO₂ mixture into thin films with an average thickness of 200 μm using an extrusion-based blade-casting method. Four films with a 0, 0.5, 1.0, and 1.5 wt % carbon nanotube were prepared. The ignition delay and flame speed of the films were measured using high-speed imaging techniques. Electrical and thermal conductivities were also measured. Results show that the inclusion of a 1.5 wt % carbon nanotube in the Mg/MnO₂/polyvinylidene fluoride films improved their flame speed by 440% and electrical conductance by two orders of magnitude (from 4.23 to 655.33 nS) and decreased ignition delay by 87.2%. Interconnectivity of carbon nanotubes in the films was estimated using a basic percolation model. Films with a 1.5 wt % carbon nanotube demonstrated the highest interconnectivity, which aided improved thermal and electrical energy transport, thereby improving combustion performance. The development of three-dimensional extruded thin films with tailorable thermal and combustion parameters is a precursor for the additive manufacturing of energetic materials.

I. Introduction

Thermite reactions are self-propagating, provide localized energy generation, high temperatures with high energy density and heat of combustion [1–3]. Since these energetic systems are mixtures of reactant powders, they can be tailored to different applications. Thus, they find versatile applications in industry and ordnance as energy-generating systems [4–10]. Although many experimental studies feature fuel and oxidizer mixtures alone, for several in-field applications, the mixtures are combined with binders to consolidate them into desirable shapes. The binders, as constituents of the energetic mixture, participate in combustion and energy transfer processes, potentially changing the behavior of the energetic system [11].

Additive manufacturing, also referred to as three-dimensional (3D) printing, is a material deposition technique that is gaining popularity [12,13] for tailoring reactants and geometry for specific applications and on demand. The processing provides systematic deposition of successive material layers by an automated system based on a premade computer model [14]. Printing enables the freedom of working with variegated material combinations, deposition of complex profiles, control of close-range features of the profiles, and decreased material wastage [15–18]. Additive manufacturing techniques like fused deposition modeling, powder bed printing, selective heat/laser sintering, and robocasting, among others, are typically employed for depositing composites [19].

Principal factors that affect the ease of printing and quality of the final product include the rheology of the binder, particulate media size distribution, thermal-physical properties of the material being deposited, and adhesion between the binder and particles [20].

Additive manufacturing may be an attractive method of printing thermite energetic systems due to several advantages offered by the process. The slurry deposited into the energetic system includes thermite powder (fuel, oxide, and required additives) and the binder. Given the novelty of the approach, and the immense freedom in processing, several researchers have focused on advancing additive manufacturing of energetic materials. Huang et al. [8] studied the effect of particle loading on the burn rate of thin films made of aluminum and polyvinylidene fluoride (PVDF) made via electro-spray deposition of Al/PVDF slurry. They showed that increasing the Al concentration increased the burn rate of the energetic film in air [8]. Li et al. [21] synthesized laminate composites consisting of alternating layers of Al/copper oxide between layers of PVDF through electro-spray deposition. Their results show that the as-made laminates burn better with fuel lean conditions, and the addition of PVDF improved the mechanical properties of the films. Meeks et al. [11] successfully synthesized and characterized the flame speeds of Mg/MnO₂ films with different binders. They showed that the energy release, porosity, and flame speed of the thin films varied with binder type and concentration. In a later work, Meeks et al. [22] investigated the rheological effects of varying concentrations of PVDF binder and film thicknesses on the flame speed and heat of combustion of Mg/MnO₂ thin films. Their results showed that flame speed increased with film thickness but decreased with increased deposition viscosity in the energetic system. Clark et al. [7] synthesized freestanding flexible 3D printable films of Al and molybdenum trioxide with silicone binder using a blade-casting approach and characterized reactivity. With binders, all of these studies produced extrudable materials that have the potential to be 3D printed, and all produced flame speeds on the order of centimeters/second.

Thermite reaction rates are dependent on a number of factors such as the particle diameter, equivalence ratio, binder concentration, homogeneity of mixing, and compaction density. Although research on additive manufacturing of energetic materials is growing, there is a need to identify mechanisms that tailor principal combustion characteristics like flame speed and ignition sensitivity for prescribed applications. A viable approach to effectively transform the combustion

Received 2 June 2016; revision received 27 September 2016; accepted for publication 17 November 2016; published online 16 February 2017. Copyright © 2016 by the American Institute of Aeronautics and Astronautics, Inc. All rights reserved. All requests for copying and permission to reprint should be submitted to CCC at www.copyright.com; employ the ISSN 0887-8722 (print) or 1533-6808 (online) to initiate your request. See also AIAA Rights and Permissions www.aiaa.org/randp.

*Graduate Research Assistant, Department of Mechanical Engineering, MS 1021; dylan.smith@ttu.edu.

†Undergraduate Research Assistant, Department of Mechanical Engineering, MS 1021; jesus.cano@ttu.edu.

‡J. W. Wright Regents Endowed Chair Professor, Department of Mechanical Engineering, MS 1021; michelle.pantoya@ttu.edu.

§Assistant Professor, Department of Mechanical Engineering, 249A Stocker Center; kappagan@ohio.edu (Corresponding Author).

characteristic of energetic systems is to introduce additives into the reactant system [1]. Additives are components of the energetic system that may not radically change reaction chemistry but influence targeted properties. One additive gaining popularity for use in thermite systems is carbon nanotubes (CNTs), which have been shown to influence thermal conductivity and diffusivity, impact sensitivity, electrostatic discharge (ESD) sensitivity, electrical conductivity, optical ignition sensitivity, and flame speeds of loose powder and compacted pellets of energetic materials [23–25].

The current work examines combustion of 3D extruded Mg/MnO₂ thin films with varying CNT concentration. Energetic thin films made of Mg/MnO₂ have been developed for use as heat sources in many applications such as thermal batteries and welding and joining [11]. Traditionally available methods of externally applied heat do not suit many applications like batteries or electronics, thus requiring the development of new and precise approaches. Energetic films inserted at a required location that can supply precise energy for a desired time are an appealing option. This particular energetic system has been chosen as the vehicular matrix to hold the CNT additives in varying concentrations and has been studied for thermal battery applications recently [11,22].

Energy transfer mechanisms depend on several factors such as material confinement, the gas products generated, the heat transfer mechanism (i.e., conduction or convection), the activation energy of the reactive components, the heating rate, and material or additive connectivity. Zhu et al. [26] examined the effects of opposed (conduction dominant) and concurrent (convection dominant) flow in thermally thin films, in which thermal thickness implies significant heat transfer through the solid phase. Meeks et al. [11] showed that Mg/MnO₂ films propagate energy conductively in open test configurations. Armstrong [23] modeled flame speeds through random particulate media with no gas generation and demonstrated that thermophysical properties of the matrix are key parameters controlling the flame speed in the second-order reaction dynamics of the global combustion reaction. Particles such as CNTs have been shown to influence the thermal [24] and electrical properties of composites [25,27]. Thus, the current work will investigate percolation in thermal and electrical properties of 3D extruded Mg/MnO₂/CNT thin films and the corresponding flame speed and ignition delay during combustion. Effective energy transfer pathways in the energetic films are examined, and factors with the greatest influence on the flame speed and ignition delay are identified. This is an extension of AIAA conference proceedings that linked electrical conductivity to flame speed but did not consider thermal property variations or provide a percolation analysis to assess CNT connectivity [27]. These are important additions that highlight the role of CNT percolation in controlling electrical, thermal, and, therefore, combustion properties [28].

II. Experimental

Micrometer size particles of Mg and MnO₂ with a 325 mesh, procured from Alfa Aesar, were used as fuel and oxidizer, respectively. Multiwalled CNTs were obtained from Alfa Aesar and were 0.1–10 μm long with a 20 nm outer diameter and 3 nm inner diameter. The energetic mixture comprising Mg and MnO₂ was prepared to have a stoichiometric equivalence ratio. Four types of energetic thin films were prepared such that they each had 0, 0.5, 1.0, and 1.5 wt % CNTs, respectively, in addition to identical quantities of the Mg/MnO₂. To cast the powders as thin films, 15 wt % PVDF was used as the binder. Requisite amounts of Mg, MnO₂, CNTs, and PVDF were mixed using methyl pyrrolidone (NMP) as the solvent such that the solids concentration of the slurry was 40 vol %. Each slurry was mixed in an AR250 Thinky centrifugal mixer at 1200 rpm for 4 min and blade cast onto a glass substrate, using a 200 μm drawdown blade with an Elcometer 4340 automated film applicator to obtain films with an average solids density of 2.1 g/cm³. The process is schematically illustrated in Fig. S1 in the Supplementary Material of this manuscript. Films were vacuum dried in an oven at 60°C for 24 h to ensure that all NMP evaporated, and then films were reclaimed for further experimentation.

Figure S2 (in the Supplementary Material) shows a schematic of the flame speed measurement setup. The rectangular films were cut to 3 mm by 3 cm strips and fixed to a glass slide placed in a pressurized combustion vessel with an argon environment at 66.6 kPa. Combustion was initiated using a small gage resistive heating wire in direct contact with the film. A Phantom v7 high-speed camera, situated perpendicular to the flame front direction, captured the thermal event. The camera recorded at 50,000 frames/s with a resolution of 512 × 384 using a 32 f-stop (i.e., $f/32$) and neutral density filters to block 92% of emitted light from the camera sensors and enable clear visualization of the flame front during propagation. The data were postprocessed using a custom Labview program. The program tracks the position of the flame front as it progresses through the film in subsequent frames and the time elapsed in between to calculate speed. The time lag between supplying resistance heating to the wire and the initiation of the reaction in the films, as witnessed from the high-speed imaging experiments, is measured as ignition delay.

Figure S3 (in the Supplementary Material) shows a schematic of the test apparatus for measuring electrical conductivity. An acrylic channel containing the energetic powder was positioned between two copper electrodes and placed inside a conductive shield to negate charges from the surroundings. An Alpha Labs high-resistance, low-conductance (HRLC) HR2 meter was connected to the two copper probes. The shielding container was held at ground potential by connecting it to the HRLC meter, which contained a high impedance amplifier. The HRLC measures a wide range of resistances varying from 1.0 Ω to 2.0 TΩ. The meter passed current through the sample at voltages below 2.0 V, which was decreased by a factor of 10 for each of the nine resistance settings. The resistance measured was then inverted to determine the conductance of the energetic samples. All the experiments were run in triplicate to assess repeatability. Uncertainty is attributed to differences in weighing, blade casting, and the accuracy of the measurement device [HRLC and laser flash analyzer (LFA)], all of which are less than the standard deviation from the repeatability of the measurements.

A Netzsch LFA was used to determine the thermal conductivity of the reactant materials and energetic system at 25°C according to the procedure detailed in previous work [29,30]. The solid components of the energetic system were dry mixed and pressed into pellets with a diameter of 1.27 cm and thickness of 0.17 cm per dimensional requirements of the sample holder of the LFA. The density of the pellets was maintained at 2.1 g/cc. Five measurements were made of each sample to determine the standard deviation from the sample measurement. The Netzsch Proteus software was used for analysis and postprocessing of the data.

III. Results

Figures 1 and 2 show the ignition delay and flame speed of the energetic films of Mg/MnO₂/PVDF as a function of CNT concentration. Figure 1 shows the ignition delay decreased from 0.68 to 0.088 ms (i.e., by 87.2%). However, as soon as the CNT was added, the ignition delay was reduced and did not vary significantly with CNT concentration. Figure 3 shows that as CNT concentration increased from 0 to 1.5 wt % flame speed increased from 67.1 to 362.5 mm/s, i.e., by 440%. The trend shows a significant increase between 1 and 1.5 wt % CNTs, suggesting the percolation of CNT particles may contribute to enhanced flame speeds. The error bars through the data symbols in Figs. 1 and 2 include error bars that represent standard deviations in the average measurement based on the repeatability of five tests per sample, and this is the largest source of uncertainty in the data collection.

Figure 4 shows adding CNTs to Mg/MnO₂/PVDF improves electrical conductance from 4.23 to 655.33 nS, which is an increase in two orders of magnitude. A similar trend is seen in Fig. 2 with flame speeds where increasing CNT concentration from 1.0 to 1.5 wt % led to a threefold increase in flame speed. Conversely, adding only 0.5 wt % CNTs (as seen in Fig. 1) decreased the ignition delay to 0.06 ms, and further addition of CNTs did not contribute further to a decreased ignition delay.

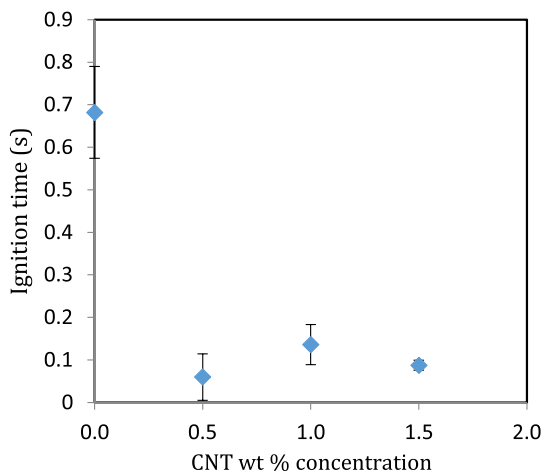


Fig. 1 Ignition delay of Mg/MnO₂/PVDF films as a function of CNT concentration. Ignition source is a resistively heated wire (i.e., thermal ignition).

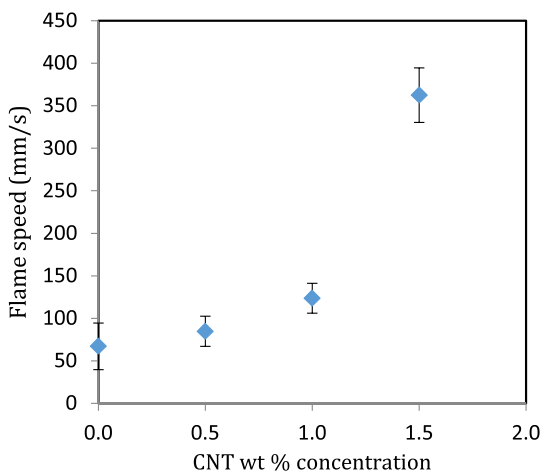


Fig. 2 Flame speed of Mg/MnO₂/PVDF films as a function of CNT concentration.

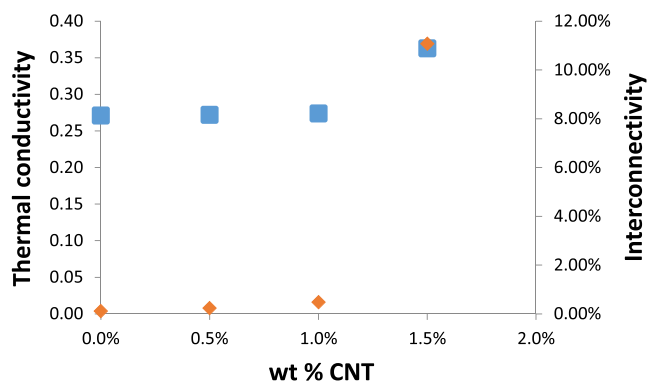


Fig. 3 Measured thermal conductivity in W/mK (square symbols) and calculated interconnectivity (diamonds) for Mg/MnO₂/PVDF films as a function of CNT concentration.

Figure 3 shows the thermal conductivity of the energetic samples as a function of CNT concentration.

IV. Discussion

The ignition delay (Fig. 1) did not follow the same trend as the flame speed, thermal or electrical conductance, or connectivity (Figs. 2–4). Ignition delay was highest in the films with no CNTs, lowered by 0.6 s at 0.5 wt % CNT concentration, and did not significantly change with a higher CNT concentration. To understand

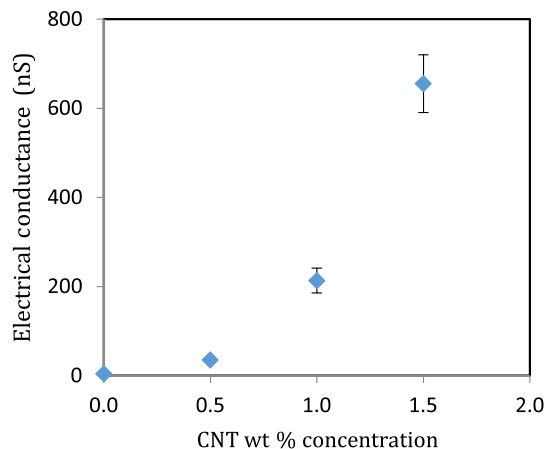


Fig. 4 Electrical conductance of Mg/MnO₂/PVDF films as a function of CNT concentration.

these trends in ignition delay, the phenomenon of ignition via resistive heating was explored further. To ignite the films, current was passed through the bent wire such that a hot spot was formed at the wire bend. The electrical and thermal energy from localized wire heating was transported to the film, which aided in initiating the combustion reaction. The rate at which energy from the wire was transported to the film depended on the energy transfer pathways between the wire bend and the film. In Mg/MnO₂/PVDF with CNTs, the CNT particles formed a well-connected pathway between the wire and film facilitating energy transport, shown in Fig. 3 and 4, by increasing the film's thermal and electrical conductivity. Even with low interconnectivity, CNTs conducted enough electrical and thermal energy for the reactants to reach an activation energy faster than films with no CNTs and thus lowered the ignition delay as seen in Fig. 1. The results show that even low concentrations of CNT additives significantly enhanced ignition sensitivity by reducing the ignition delay time when exposed to an energy source. Additional particle connectivity was not required to sensitize the composite to ignition, and small variations in bulk thermal and electrical properties (Figs. 3 and 4) correlate with significant variations in ignition sensitivity (Fig. 1).

Figure 2 shows flame speeds increased exponentially from 67.1 mm/s with 0.0 wt % CNTs to 362.5 mm/s (i.e., a 440% increase) with 1.5 wt %. The increase in flame speed was facilitated by the increase in thermal conductivity of the films (Fig. 3) and followed the same exponential trend. The relatively slow speed (i.e., mm/s) and the open configuration of the test setup suggested the dominant mode of heat transfer was thermal conduction. Although Mg/MnO₂ did not generate gas [11], PVDF decomposition and burning are gas phase reactions. However, generated gas escaped the reaction zone without confinement and did not contribute to convective energy transport within the film, especially evident by the slow propagation of the reaction in the condensed phase (i.e., millimeters/second). This shows that increasing thermal conductivity of thin films will increase flame speeds for conductively driven reactions.

Because the additive exponentially influenced thermal and combustion properties of the composite, the threshold concentration for percolation was examined. The lowest concentration that would provide enhanced thermal behavior can be identified using a percolation analysis. Schilling and Partzsch [31] and Weidenfeller et al. [32] used interconnectivity as a way to quantify the connectivity between particles as their concentration in a composite increased. First, they estimated the volume fraction of the filler-additive and constituent matrix, as Φ_F and Φ_M , respectively. Then, using the thermal conductivity of the additive λ_F and matrix λ_M , the theoretical upper bound λ^{HS+} and lower bound λ^{HS-} of thermal conductivity were calculated using Eqs. (1) and (2) [29]:

$$\lambda^{HS+} = \lambda_F \frac{2\lambda_F + \lambda_M - 2\phi_M(\lambda_F - \lambda_M)}{2\lambda_F + \lambda_M + 2\phi_M(\lambda_F - \lambda_M)} \quad (1)$$

$$\lambda^{\text{HS-}} = \lambda_M \frac{2\lambda_M + \lambda_F - 2\phi_F(\lambda_M - \lambda_F)}{2\lambda_M + \lambda_F + 2\phi_F(\lambda_M - \lambda_F)} \quad (2)$$

The interconnectivity of the additive in the composite was calculated based on the measured thermal conductivity λ_{MD} according to Eq. (3):

$$X = \frac{\lambda_{\text{MD}} - \lambda^{\text{HS-}}}{\lambda^{\text{HS+}} - \lambda^{\text{HS-}}} \quad (3)$$

Interconnectivity quantifies how connected particles are such that $X = 1$ would correspond to complete 100% connectivity while $x = 0.5$ would imply half the additive particles form a connected network through the matrix. Equation (3) shows that the thermal conductivity of the bulk film is dependent on the morphology of the particles, the bulk density (indicating the amount of void space occupied by air), and the thermal conductivity of the constituents of the films (i.e., Mg, MnO_2 , PVDF, and air). These are combined in the interconnectivity equation and referred to as the matrix. As long as concentrations of the matrix constituents and density of the samples are held constant, the thermal conductivity of the matrix can be determined by LFA measurements. The LFA analysis quantifies the increase in thermal conductivity caused specifically by the additive concentration. This equation is most often used to describe thermal conductivity because there is a dramatic difference between additive thermal conductivity and matrix conductivity in polymer composites.

Using this approach, the interconnectivity X of the CNT in $\text{Mg}/\text{MnO}_2/\text{PVDF}$ film was calculated and is shown in Fig. 3. There was a dramatic increase in interconnectivity when the CNT concentration increased from 1.0 to 1.5 wt %, suggesting percolation [29]. Previous research [29] showed that interconnectivity and electrical conductivity are closely related. Whereas the interconnected additive pathways facilitate energy transport in general, at the inflection point, there will be a more significant increase in electrical conductivity than thermal conductivity. The same trend is mirrored here and seen by the 150 times increase in electrical conductance (see Fig. 4) compared to the three times increase in flame speed (see Fig. 2).

Furthermore, the estimated interconnectivity of CNTs in the films (see Fig. 3) shows that using a standard rule of averages is not an accurate approach for estimating thermal conductivity [29]. This is because there is a natural assumption in a weighted average approach that the composite is fully connected ($X = 1$). The additive shape, particle size distribution, and density all have an effect on interconnectivity that is not accounted for in a weighted average approach. Interconnectivity has a more significant influence on energy transport than the average conductivity of the composite components.

V. Conclusions

The influence of carbon nanotubes (CNTs) on the flame speed, ignition delay, thermal conductivity, and electrical conductance of energetic films composed of $\text{Mg}/\text{MnO}_2/\text{polyvinylidene flouride}$ with varying concentrations of CNT additives were studied. A CNT particle connectivity analysis was also performed to identify the role of percolation affecting thermal and electrical behavior. Results show that ignition delay times were significantly reduced even with low concentrations of CNTs and remained unchanged with increasing CNT concentration. This implies that sensitizing a composite toward thermal ignition can be achieved with small concentrations (i.e., less than 1 wt %) and without additive percolation. Further results show that adding CNTs improved the flame speed of the energetic thin films by 440% and electrical conductance by two orders of magnitude and significantly affected thermal conductivity at percolation. Films had the highest interconnectivity of CNTs when added at 1.5 wt %, which corresponded with an exponential increase in the flame speed and interconnectivity. Increased energy transport pathways in the composite energetic films due to improved interconnectivity of the CNTs allowed faster and more efficient thermal energy transfer through the film resulting in higher flame speeds with a higher

interconnectivity of CNTs. Thus, interconnectivity (and percolation) of CNTs was identified as a key factor in explaining the improved flame speed of the energetic films with additives and the decrease in their ignition delay.

Acknowledgments

The authors are thankful for support from the U.S. Army Research Office grant number W911NF-14-1-0250 and encouragement from their program manager, Ralph Anthenien.

References

- [1] Kappagantula, K., Crane, C., and Pantoya, M., "Factors Influencing Temperature Fields During Combustion Reactions," *Propellants, Explosives, Pyrotechnics*, Vol. 39, No. 3, 2014, pp. 434–443. doi:10.1002/prep.201300154
- [2] Cheng, J. L., Hng, H. H., Lee, Y. W., Du, S. W., and Thadhani, N. N., "Kinetic Study of Thermal- and Impact-Initiated Reactions in Al-Fe2O3 Nanothermite," *Combustion and Flame*, Vol. 157, No. 12, 2010, pp. 2241–2249. doi:10.1016/j.combustflame.2010.07.012
- [3] Granier, J. J., and Pantoya, M. L., "Laser Ignition of Nanocomposite Thermites," *Combustion and Flame*, Vol. 138, No. 4, 2004, pp. 373–383. doi:10.1016/j.combustflame.2004.05.006
- [4] Glavier, L., Taton, G., Duc  r  , J.-M., Baijot, V., Pinon, S., Calais, T., Est  ve, A., Djafari Rouhani, M., and Rossi, C., "Nanoenergetics as Pressure Generator for Nontoxic Impact Primers: Comparison of Al/Bi2O3, Al/CuO, Al/MoO3 Nanothermites and Al/PTFE," *Combustion and Flame*, Vol. 162, No. 5, 2015, pp. 1813–1820. doi:10.1016/j.combustflame.2014.12.002
- [5] Rossi, C., Zhang, K., and Esteve, D., "Nanoenergetic Materials for MEMS: A Review," *Journal of Microelectromechanical Systems*, Vol. 16, No. 4, 2007, pp. 919–931.
- [6] Sullivan, K. T., Wu, C., Piekielek, N. W., Gaskell, K., and Zachariah, M. R., "Synthesis and Reactivity of Nano-Ag2O as an Oxidizer for Energetic Systems Yielding Antimicrobial Products," *Combustion and Flame*, Vol. 160, No. 2, 2013, pp. 438–446. doi:10.1016/j.combustflame.2012.09.011
- [7] Clark, B., McCollum, J., Pantoya, M. L., Heaps, R. J., and Daniels, M. A., "Development of Flexible, Free-Standing, Thin Films for Additive Manufacturing and Localized Energy Generation," *AIP Advances*, Vol. 5, No. 8, 2015, Paper 087128. doi:10.1063/1.4928570
- [8] Huang, C., Jian, G., DeLisio, J. B., Wang, H., and Zachariah, M. R., "Electrospray Deposition of Energetic Polymer Nanocomposites with High Mass Particle Loadings: A Prelude to 3D Printing of Rocket Motors," *Advanced Engineering Materials*, Vol. 17, No. 1, 2015, pp. 95–101. doi:10.1002/adem.201400151
- [9] Clayton, N. A., Kappagantula, K. S., Pantoya, M. L., Kettwich, S. C., and Iacono, S. T., "Fabrication, Characterization, and Energetic Properties of Metallized Fibers," *ACS Applied Materials and Interfaces*, Vol. 6, No. 9, 2014, pp. 6049–6053. doi:10.1021/am404583h
- [10] Kettwich, S. C., Kappagantula, K., Kusel, B. S., Avjian, E. K., Danielson, S. T., Miller, H. A., Pantoya, M. L., and Iacono, S. T., "Thermal Investigations of Nanoaluminum/Perfluoropolyether Core-Shell Impregnated Composites for Structural Energetics," *Thermochimica Acta*, Vol. 591, Sept. 2014, pp. 45–50. doi:10.1016/j.tca.2014.07.016
- [11] Meeks, K., Pantoya, M. L., and Apblett, C., "Deposition and Characterization of Energetic Thin Films," *Combustion and Flame*, Vol. 161, No. 4, 2014, pp. 1117–1124. doi:10.1016/j.combustflame.2013.10.027
- [12] Lipson, H., and Kurman, M., *Fabricated: The New World of 3D Printing: Books*, Wiley, Hoboken, NJ, 2013, pp. 1–25.
- [13] Lin, D., Nian, Q., Deng, B., Jin, S., Hu, Y., Wang, W., and Cheng, G. J., "Three-Dimensional Printing of Complex Structures: Man Made or Toward Nature?" *ACS Nano*, Vol. 8, No. 10, 2014, pp. 9710–9715. doi:10.1021/nn504894j
- [14] Sachs, E., Cima, M., Cornie, J., Brancazio, D., Bredt, J., Curodeau, A., Fan, T., Khanuja, S., Lauder, A., Lee, J., and Michaels, S., "Three-Dimensional Printing: The Physics and Implications of Additive Manufacturing," *CIRP Annals — Manufacturing Technology*, Vol. 42, No. 1, 1993, pp. 257–260. doi:10.1016/S0007-8506(07)62438-X
- [15] Vaezi, M., Seitz, H., and Yang, S., "A Review on 3D Micro-Additive Manufacturing Technologies," *International Journal of Advanced*

- Manufacturing Technology*, Vol. 67, Nos. 5–8, 2013, pp. 1721–1754.
doi:10.1007/s00170-012-4605-2
- [16] Li, L., Saedan, M., Feng, W., Fuh, J. Y. H., Wong, Y. S., Loh, H. T., Thian, S. C. H., Thoroddsen, S. T., and Lu, L., “Development of a Multi-Nozzle Drop-on-Demand System for Multi-Material Dispensing,” *Journal of Material Processing Technology*, Vol. 209, No. 9, 2009, pp. 4444–4448.
doi:10.1016/j.jmatprotec.2008.10.040
- [17] Torrado Perez, A. R., Roberson, D. A., and Wicker, R. B., “Fracture Surface Analysis of 3D-Printed Tensile Specimens of Novel ABS-Based Materials,” *J. Fail. Anal. Prev.*, Vol. 14, No. 3, 2014, pp. 343–353.
doi:10.1007/s11668-014-9803-9
- [18] Postiglione, G., Natale, G., Griffini, G., Levi, M., and Turri, S., “Conductive 3D Microstructures by Direct 3D Printing of Polymer/Carbon Nanotube Nanocomposites via Liquid Deposition Modeling,” *Composites Part A: Applied Science and Manufacturing*, Vol. 76, Sept. 2015, pp. 110–114.
doi:10.1016/j.compositesa.2015.05.014
- [19] Wong, K. V., and Hernandez, A., “A Review of Additive Manufacturing,” *ISRN Mechanical Engineering*, Vol. 2012, 2012, pp. 1–10.
doi:10.5402/2012/208760
- [20] Guo, N., and Leu, M. C., “Additive Manufacturing: Technology, Applications and Research Needs,” *Frontiers of Mechanical Engineering*, Vol. 8, No. 3, 2013, pp. 215–243.
doi:10.1007/s11465-013-0248-8
- [21] Li, X., Guerieri, P., Zhou, W., Huang, C., and Zachariah, M. R., “Direct Deposit Laminate Nanocomposites with Enhanced Propellant Properties,” *ACS Applied Materials and Interfaces*, Vol. 7, No. 17, 2015, pp. 9103–9109.
doi:10.1021/acsami.5b00891
- [22] Meeks, K. A., Clark, B. R., Cano, J. E., Apblett, C. A., and Pantoya, M. L., “Effects of Rheological Properties on Reactivity of Energetic Thin Films,” *Combustion and Flame*, Vol. 162, No. 9, 2015, pp. 3288–3293.
doi:10.1016/j.combustflame.2015.05.018
- [23] Armstrong, R., “Models for Gasless Combustion in Layered Materials and Random Media,” *Combustion Science and Technology*, Vol. 71, Nos. 4–6, June 1990, pp. 155–174.
doi:10.1080/00102209008951630
- [24] Bakshi, S. R., Lahiri, D., and Agarwal, A., “Carbon Nanotube Reinforced Metal Matrix Composites: A Review,” *International Materials Reviews*, Vol. 55, No. 1, 2010, pp. 41–64.
doi:10.1179/0950666009X12572530170543
- [25] Steelman, R., Clark, B., Pantoya, M. L., Heaps, R. J., and Daniels, M. A., “Desensitizing Nano Powders to Electrostatic Discharge Ignition,” *Journal of Electrostatics*, Vol. 76, Aug. 2015, pp. 102–107.
doi:10.1016/j.elstat.2015.05.008
- [26] Zhu, F., Lu, Z., and Wang, S., “Flame Spread and Extinction over a Thick Solid Fuel in Low-Velocity Opposed and Concurrent Flows,” *Microgravity Science and Technology*, Vol. 28, No. 2, 2016, pp. 87–94.
doi:10.1007/s12217-015-9475-4
- [27] Collins, E. S., Skelton, B. R., Pantoya, M. L., Irin, F., Green, M. J., and Daniels, M. A., “Ignition Sensitivity and Electrical Conductivity of an Aluminum Fluoropolymer Reactive Material with Carbon Nanofillers,” *Combustion and Flame*, Vol. 162, No. 4, 2015, pp. 1417–1421.
doi:10.1016/j.combustflame.2014.11.008
- [28] Kappagantula, K. S., Cano, J., and Pantoya, M. L., “Combustion Performance Improvement of Energetic Thin Films Using Carbon Nanotubes,” *51st AIAA/SAE/ASEE Joint Propulsion Conference, Propulsion and Energy Forum*, AIAA Paper- 2015-3909, 2015.
- [29] Smith, D. K., and Pantoya, M. L., “Effect of Nanofiller Shape on Effective Thermal Conductivity of Fluoropolymer Composites,” *Composites Science and Technology*, Vol. 118, Oct. 2015, pp. 251–256.
doi:10.1016/j.compscitech.2015.09.010
- [30] Kappagantula, K., and Pantoya, M. L., “Experimentally Measured Thermal Transport Properties of Aluminum? Polytetrafluoroethylene Nanocomposites with Graphene and Carbon Nanotube Additives,” *International Journal of Heat and Mass Transfer*, Vol. 55, No. 4, 2012, pp. 817–824.
doi:10.1016/j.ijheatmasstransfer.2011.10.026
- [31] Schilling, F. R., and Partzsch, G. M., “Quantifying Partial Melt Fraction in the Crust Beneath the Central Andes and the Tibetan Plateau,” *Physics and Chemistry of the Earth, Part A: Solid Earth and Geodesy*, Vol. 26, No. 4, 2001, pp. 239–246.
- [32] Weidenfeller, B., Höfer, M., and Schilling, F., “Thermal and Electrical Properties of Magnetite Filled Polymers,” *Composites Part A: Applied Science and Manufacturing*, Vol. 33, No. 8, 2002, pp. 1041–1053.
doi:10.1016/S1359-835X(02)00085-4